The Impact of the Topology on the Throughput of Interference-limited Sensor Networks with Rayleigh Fading

Xiaowen Liu and Martin Haenggi
University of Notre Dame
Department of Electrical Engineering
Notre Dame, IN 46556, USA
{xliu4, mhaenggi}@nd.edu

***Abstract*— In this paper, we present closed-form expressions of the average per-node throughput for sensor networks with a slotted ALOHA MAC protocol in Rayleigh fading channels. We compare networks with three regular topologies in terms of per-node throughput, transmit efficiency, and transport capacity. In particular, for square lattice networks, we present an analysis of the dependence of the maximum throughput and optimum transmit probability on the signal-to-interference-ratio threshold required for successful reception. For random networks with nodes distributed according to a two-dimensional Poisson point process, the average per-node throughput is analytically characterized and numerically evaluated. It turns out that although regular networks have an only slightly higher per-node throughput than random networks for the same link distance, regular topologies have a significant benefit when the end-to-end throughput in multihop connections is considered.**

I. Introduction

A sensor network [1] consists of a large number of sensor nodes which are placed inside or near a phenomenon. Uniformly random or Poisson distributions are widely accepted models for the location of the nodes in wireless sensor networks, if nodes are deployed in large quantities and there is little control over where they are dropped. A typical scenario is a deployment from an airplane for battlefield monitoring. On the other hand, depending on the application, it may also be possible to place sensors in a regular topology, for example in a square grid.

Throughput is a traditional measure of how much traffic can be delivered by the network [2], [3]. There is a rich literature on throughput capacity for wireless networks [2], [4], [5] with random or regular topologies. The seminal paper [2] shows that, under certain assumptions, in a static two-dimensional network with N nodes and $N/2$ randomly selected source-destination pairs, the end-to-end throughput of a connection is at most $\Theta(W/\sqrt{N})$, where W is the maximum transmission rate for each node. However, such "order of" results do not provide any guidelines for protocol design, since the scaling behavior is very robust against changes in MAC and routing protocols [6]. All the above research work assumes networks with randomly located nodes. There are also research efforts focusing on networks with regular topologies which allow for mathematical tractability and provide valuable insight. [4] calculates the throughput of a regular square networks with a slotted ALOHA channel access scheme. [6] proves that the $\Theta(N)$ upper bound on transport capacity is tight for regular square networks with path loss exponents greater than 3. [7] compares the performance of regular topologies with random topology in wireless CDMA sensor networks. [8] and [9] evaluate the performance for regular grid and random topologies. They assume a "torus" network to avoid boundary effects and use the expected interference power to replace the exact interference power. In particular at high load, replacing the actual interference by its mean yields overly pessimistic results.

Most of the work above is based on a "disk model", where it is assumed that the radius for a successful transmission of a packet has a fixed and deterministic value, irrespective of the condition and the realization of the wireless channel. Such simplified link models

The support of the U.S. National Science Foundation (grants ECS 03-29766 and CAREER CNS 04-47869) is gratefully acknowledged.

ignore the stochastic nature of the wireless channel. Our analysis is based on a Rayleigh fading channel model, which includes both large-scale path loss and stochastic small-scale variations in the channel characteristics. Note that even with static nodes as assumed in this paper, the channel quality varies because any movement in the environment affects the multipath geometry of the RF signal, which is easily confirmed experimentally [10, p. 45]. The significant variation of the link quality when nodes are immobile is also pointed out in [11]–[13], and the shortcomings of the "disk model" are discussed in [14].

This paper addresses the throughput problem for large sensor networks with Rayleigh fading channels. To provide insight on the impact of the topology on the networks performance, we compare networks with a random and three regular topologies. We define the throughput as the expected number of successful packet transmissions of a given node per timeslot. The *end-to-end* throughput over a multihop connection, defined as the minimum of the throughput values of the nodes involved, is a performance measure of a route and the MAC scheme. It is assumed that every node always has a packet to transmit (heavy traffic) and that all the networks have the same density $\lambda = 1$.

We consider slotted ALOHA [4], which is a simple random access scheme often used. It assumes that in every timeslot, every node transmit with probability p. The traffic distribution in a sensor networks is usually spatially and temporally bursty, *i.e.*, busy periods alternate temporally and busy areas alternate spatially with periods and areas with little or no traffic. It may therefore be impractical to employ reservation-based MAC schemes such as TDMA and FDMA that require a substantial amount of coordination traffic and cannot be implemented efficiently and in a fully distributed fashion[1]. In any case, the slotted ALOHA scheme is the simplest meaningful MAC scheme and therefore provides a lower bound on the performance for more elaborate schemes. Since areas of the network or periods with little or no traffic pose no problems, our analysis focuses on and applies to busy areas and busy periods of the network where collisions are unavoidable and the throughput is interference-limited.

In Section II, the Rayleigh fading link model is introduced, For a slotted ALOHA MAC scheme, the conditional success probability of a transmission for a node given the transmitter-receiver and interference-receiver distances is derived. Section III evaluates the (per-node) throughput for networks with three regular topologies and compares their performance. In particular, for square networks, the analysis of the dependence of the maximum throughput and the optimum transmit probability on signal-to-interference-ratio threshold (SIR) Θ is provided. Section IV investigates the average throughput for random networks with and without given transmitter-receiver distance d_0. This section also analyzes the transport capacity and end-to-end throughput. Section V concludes the paper.

[1]In general this problem is NP-hard.

II. The Rayleigh Fading Link Model

We assume a flat Rayleigh block fading channel. A transmission from node i to node j is successful if the signal-to-noise-and-interference ratio (SINR) γ_{ij} is above a certain threshold Θ that is determined by the communication hardware and the modulation and coding scheme [12]. The SINR γ is given by $\gamma = \frac{Q}{N_0+I}$, where Q is the received power, which is exponentially distributed with mean $\bar{Q}$. N_0 denotes the noise power, and I is the interference power, *i.e.*, the sum of the received power from all the undesired transmitters. Over a transmission of distance d with an attenuation d^{α}, we have $\bar{Q} = P_0 d^{-\alpha}$, where P_0 denotes the transmit power, α is the path loss exponent. Our analysis is based on the following theorem:

Theorem 1: In a Rayleigh fading network with slotted ALOHA, where nodes transmit at equal power levels with probability p, the success probability of a transmission given a desired transmitter-receiver distance d_0 and n other nodes at distances d_i ($i = 1, \ldots, n$) is

$$P_{s|d_0,\ldots,d_n} = \exp\Big(-\frac{\Theta N_0}{P_0 d_0^{-\alpha}}\Big) \cdot \prod_{i=1}^{n} \Big(1 - \frac{\Theta p}{\Big(\frac{d_i}{d_0}\Big)^{\alpha} + \Theta}\Big) \quad (1)$$

where P_0 is the transmit power, N_0 the noise power, and Θ the SINR threshold.

Proof: Let Q_0 denote the received power from the desired transmitter and Q_i, $i = 1, \ldots, n$, the received power from n potential interferers. All the received powers are exponentially distributed, *i.e.*, $p_{Q_i}(q_i) = 1/\bar{Q}_i e.^{-q_i/\bar{Q}_i}$, where $\bar{Q}_i$ denotes the average received

power $\bar{Q}_i = P_i d_i^{-\alpha}$. The cumulated interference power at the receiver is

$$I = \sum_{i=1}^{n} S_i Q_i,$$

where S_i is a sequence of iid Bernoulli random variables with $\mathbb{P}(S_i = 1) = p$ and $\mathbb{P}(S_i = 0) = 1-p$. The success probability of a transmission is[2]

$$\begin{aligned}
P_{s|d_0,d_1,\ldots,d_n} &= \mathbb{E}_I\Big[\mathbb{P}[Q_0 \geqslant \Theta(I+N_0) \mid I\,]\Big] \\
&= \mathbb{E}_{Q,S}\Big[\exp\Big(-\frac{\Theta(\sum_{i=1}^{n} S_i Q_i + N_0)}{\bar{Q}_0}\Big)\Big] \\
&= \exp\Big(-\frac{\Theta N_0}{\bar{Q}_0}\Big)\mathbb{E}_{Q,S}\Big[\prod_{i=1}^{n}\exp\Big(-\frac{\Theta(S_i Q_i)}{\bar{Q}_0}\Big)\Big] \\
&= \exp\Big(-\frac{\Theta N_0}{P_0 d_0^{-\alpha}}\Big)\prod_{i=1}^{n}\Big\{P(S_i=1) \\
&\quad \cdot \int_0^{\infty}\exp\Big(-\frac{\Theta q_i}{\bar{Q}_0}\Big)p_{Q_i}(q_i)\mathrm{d}q_i + P(S_i=0)\Big\} \\
&= \exp\Big(-\frac{\Theta N_0}{P_0 d_0^{-\alpha}}\Big)\prod_{i=1}^{n}\Big(\frac{p}{1+\Theta\big(\frac{d_0}{d_i}\big)^{\alpha}} + 1 - p\Big) \\
&= \exp\Big(-\frac{\Theta N_0}{P_0 d_0^{-\alpha}}\Big)\prod_{i=1}^{n}\Big(1 - \frac{\Theta p}{\Big(\frac{d_i}{d_0}\Big)^{\alpha} + \Theta}\Big) \qquad (2)
\end{aligned}$$

■

Note that in Theorem 1, the success probability is obtained without knowing who is transmitting among the n nodes in each timeslot. We are interested in the interference-limited case, so we focus on the interference part of (2), *i.e.*, the second factor. This implies that the results obtained will have to be multiplied by the noise term that is easy to determine and therefore not included in our derivations. In addition, by increasing the transmit power, the noise term approaches 1, so our results represent MAC-dependent bounds that can be approached but not exceeded even if the transmit power were not constrained.

Corollary 2: Under the same assumptions as in Theorem 1 but with $N_0 = 0$ and unit transmit power $P_i = 1$, the success probability given a desired link of normalized distance $r_0 = d_0/d_0 = 1$ and n other nodes at normalized distances $r_i = d_i/d_0$ is:

$$P_{s|r_0,r_1,\ldots,r_n} = \prod_{i=1}^{n}\Big(1 - \frac{p}{1 + {r_i}^{\alpha}/\Theta}\Big) = \mathcal{L}_I(\Theta), \qquad (3)$$

which is the Laplace transform of the interference power I evaluated at the SIR threshold Θ.[3]

Proof: With unit transmit power, the mean power from the i-th interferer at distance r_i is $1/r_i^{\alpha}$. The Laplace transform of the exponential distribution with mean $1/\mu$ is $\mu/(\mu+s)$, thus the Laplace transform of I is [18]:

$$\begin{aligned}
\mathcal{L}_I(s) &= \prod_{i=1}^{n}\Big(\frac{p r_i^{\alpha}}{r_i^{\alpha}+s} + 1 - p\Big) \\
&= \prod_{i=1}^{n}\Big(1 - \frac{p}{1 + r_i^{\alpha}/s}\Big) \qquad (4)
\end{aligned}$$

From (2) and with $r_i = d_i/d_0$ (normalized distances), if $N_0 = 0$,

$$P_{s|r_0,r_1,\ldots,r_n} = \prod_{i=1}^{n}\Big(1 - \frac{p}{1 + {r_i}^{\alpha}/\Theta}\Big) \qquad (5)$$

we get (3). ■

III. Regular Networks

In this section, we investigate networks with three regular topologies (square, triangle, hexagon) in which every node has the same number of nearest neighbors and the distance between all pairs of nearest neighbors is the same.

A. Square networks

We first analyze square networks with N nodes placed in the vertices of a square grid with distance 1 between all pairs of nearest nodes (density 1). The next-hop receiver of each packet is one of the four nearest neighbor nodes of the transmitter, so the transmitter-receiver distance $d_0 = 1$. If the receiver node O is located in the center of the network as shown in Fig. 1 and node A is the desired transmitter, the success probability for node O based on (5) can be written as:

$$\begin{aligned}
P_s(p) &= \Big(1 - \frac{\Theta p}{1^{\alpha}+\Theta}\Big)^3 \cdot \Big(1 - \frac{\Theta p}{(\sqrt{2})^{\alpha}+\Theta}\Big)^4 \\
&\cdot \prod_{i=2}^{\sqrt{N}/2}\Big\{\Big(1 - \frac{\Theta p}{i^{\alpha}+\Theta}\Big)^4 \cdot \Big(1 - \frac{\Theta p}{(\sqrt{2i^2})^{\alpha}+\Theta}\Big)^4 \\
&\cdot \prod_{j=1}^{i-1}\Big(1 - \frac{\Theta p}{(\sqrt{i^2+j^2})^{\alpha}+\Theta}\Big)^8\Big\}. \qquad (6)
\end{aligned}$$

The first term in (6) accounts for the other three nearest

[2] A similar calculation has been carried out in [15] for a network with known simultaneously transmitting nodes.

[3] The identity between the Laplace transform of the interference and the reception probability in Rayleigh fading channels has been pointed out in [16], [17].

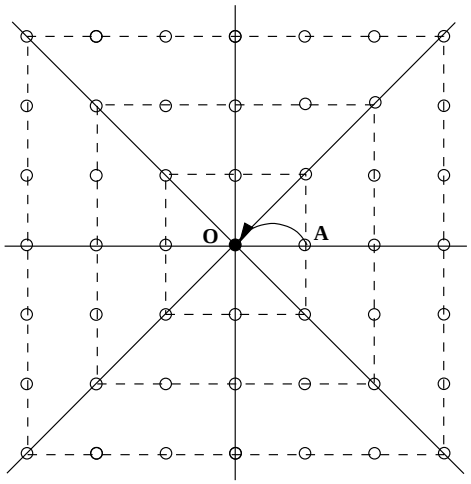

Fig. 1. The topology of a square network. Node O is the receiver and node A is the desired transmitter, where $d_0 = |OA| = 1$.

neighbor nodes of the receiver; the second term for the 4 diagonal nodes at distance $\sqrt{2}$; all the other terms from the nodes located on the dashed squares with edge ≥ 2 in Fig. 1. The throughput[4] is given by

$$g(p) = p(1-p)P_s(p), \tag{7}$$

where p is the probability that A transmits and $1-p$ is the probability that O does not transmit in the same timeslot. The analytic throughput g vs. p based on (6) and (7) for a regular square network with 40×40 nodes with node density $\lambda = 1$ is displayed in Fig. 2 (a). For $\alpha = 4$, the maximum throughput $g_{\max} = 0.0247$ is achieved at an optimal transmit probability $p_{\text{opt}} = 0.066$. The transmit efficiency, defined as $T_{\text{eff}} = g_{\max}/p_{\text{opt}}$, is 37.4%. The simulation result[5] of the throughput for a 40×40 square network is plotted in Fig. 2 (b), where for $\alpha = 4$, the maximum throughput $g_{\max} = 0.0252$ is achieved at $p_{\text{opt}} = 0.066$. It is shown that the analytic results match the simulation perfectly.

For the analysis of the throughput as a function of Θ, we need to determine $p_{\text{opt}}(\Theta)$ and $g_{\max}(\Theta)$. We use three analytic approximations to find $p_{\text{opt}}(\Theta)$ and

[4]The throughput is calculated as the throughput of the center node. This is the worst case since most other nodes experience a lower interference. In the case of infinite networks, the interference distribution is the same at every node.

[5]We use MATLAB to simulate the MAC scheme and the Rayleigh fading channel. For the simulation, we consider only the center nodes to avoid boundary effects.

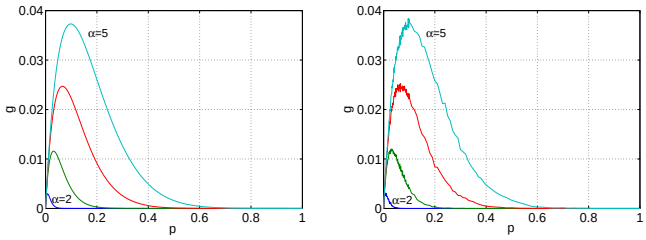

(a) (b)

Fig. 2. For a square network with 40×40 nodes, with $\Theta = 10$, (a) the analytic throughput $g(p)$ based on equation (6) and (b) the simulated throughput.

$g_{\max}(\Theta)$. From (5), g can be written as

$$g = p(1-p)\prod_{i=1}^{n}\Big(1 - \frac{p}{1 + r_i^{\alpha}/\Theta}\Big), \tag{8}$$

where $r_i = d_i/d_0$.
Since $p_{\text{opt}} = \arg\max_p g(p) = \arg\max_p \log\big(g(p)\big)$, we maximize

$$\log(g) = \log(p) + \log(1-p) + \sum_{i=1}^{n}\log\Big(1 - \frac{p}{1 + r_i^{\alpha}/\Theta}\Big), \tag{9}$$

using $\log(1+x) \approx x$ for small x,[6] yielding

$$p_{\text{opt}}^2 - p_{\text{opt}}(1+2s) + s = 0, \tag{10}$$

with

$$s = \frac{1}{\sum_{i=1}^{n}\frac{1}{1+r_i^{\alpha}/\Theta}}. \tag{11}$$

Note $r_i = d_i$ for $d_0 = 1$. So, p_{opt} is given by

$$p_{\text{opt}} = s + \frac{1}{2}\Big(1 - \sqrt{1+4s^2}\Big). \tag{12}$$

$g_{\max}$ can be written as $g_{\max} = p_{\text{opt}}(1-p_{\text{opt}})P_s(p_{\text{opt}})$, where $P_s(p_{\text{opt}})$ is obtained by plugging p_{opt} into (6), where s is given by (11). This approximation method is called *Analytic 1*. Note that the only approximation involved in the derivation of *Analytic 1* is $\log(1+x) \approx x$.

For $\alpha = 4$, we use i^2 to approximate d_i^4 for the nodes located in one quadrant. As shown in Fig. 3, the distance of node i ($i = 1, \ldots, 8$) in the first quadrant to the receiver node O is d_i. Table I compares d_i^4 and i^2 for $i = 1, \ldots, 8$. By Euler's summation formula, $d_i^4 \approx i^2$

[6]The approximation is accurate for small p in the range of interest, *i.e.*, $0 < p < 0.3$.

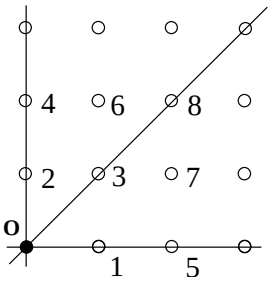

Fig. 3. Node numbering scheme pertaining to Table I for nodes in the first quadrant of a square network. O is the receiver.

TABLE I
COMPARISON OF d_i^4 AND i^2.

i	1	2	3	4	5	6	7	8
d_i^4	1	1	4	16	16	25	25	64
i^2	1	4	9	16	25	36	49	64

allows a simplification (the node at distance 1 is the desired transmitter):

$$\sum_{i=2}^{k+1} \frac{1}{1+i^2/\Theta} \approx \sqrt{\Theta}\Big(\arctan\frac{k+3/2}{\sqrt{\Theta}} - \arctan\frac{3}{2\sqrt{\Theta}}\Big). \tag{13}$$

For $k \to \infty$,

$$s \approx \frac{1}{4\sqrt{\Theta}\Big(\frac{\pi}{2} - \arctan\frac{3}{2\sqrt{\Theta}}\Big)}, \tag{14}$$

where 4 in (14) comes from the fact that nodes are located in 4 quadrants. Plugging (14) into (12) is our method *Analytic 2*.

In method *Analytic 3*, we use the approximation $s \approx 1/(4\sqrt{\Theta})$, which is within $\mp 20\%$ for the practical range $9/(2\cot(0.8))^2 \approx 2.4 < \Theta < 9/(2\cot(1.2))^2 \approx 14.9$, and substitute it into (12),

$$p_{\text{opt}} = \frac{1}{4\sqrt{\Theta}} + \frac{1}{2}\Big(1 - \sqrt{1+\frac{1}{4\Theta}}\ \Big). \tag{15}$$

Based on (9) and (11), $g_{\max}$ is given by

$$g_{\max} = p_{\text{opt}}(1-p_{\text{opt}})\ e^{-p_{\text{opt}}/s}. \tag{16}$$

The numerical result obtained by direct maximization of (6) for different Θ is compared with the results from the three analytical approximations in Fig. 4. In *Analytic 2*, approximating interfering nodes at distance d_i by the larger distance $i^{1/2}$ (shown in Table I) results in lower interference. The interference has a more significant

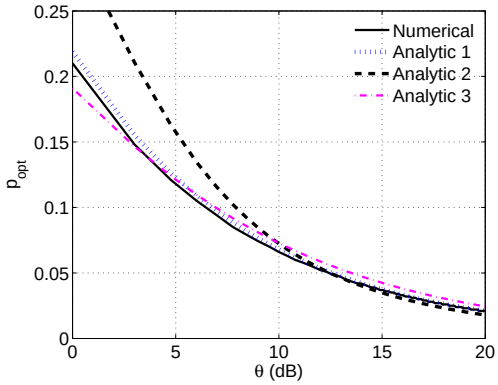

(a)

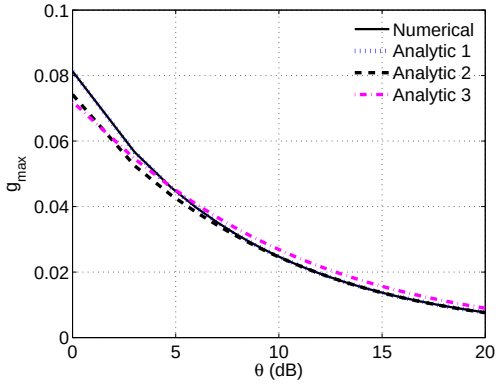

(b)

Fig. 4. For a square network with 40×40 nodes and $\alpha = 4$, the numerical results and analytic results from *Analytic 1*, *Analytic 2* and *Analytic 3* for (a) the relationship between p_{opt} and Θ; (b) the relationship between $g_{\max}$ and Θ.

impact on the throughput (thus p_{opt}) for small Θ (see (13)). Thus for small Θ, this lower interference leads to a higher p_{opt} than for *Analytic 1*. The transmit efficiency is $T_{\text{eff}} = g_{\max}/p_{\text{opt}} = (1-p_{\text{opt}})e^{-p_{\text{opt}}/s}$, which is monotonically increasing from $\lim_{s\to 0} T_{\text{eff}} = e^{-1} \approx 0.37$ to $\lim_{s\to\infty} T_{\text{eff}} = 1/2$. The upper bound is achieved if the interference goes to zero, in which $p_{\text{opt}} = 1/2$ and $g_{\max} = 1/4$. For the lower bound, as $s \to 0$, we have $p_{\text{opt}} \to 0$ and $g_{\max} \to 0$, and T_{eff} converges to e^{-1}. Hence s is a measure for spatial reuse. Indeed for $s \to 0$, which happens for $\alpha \to 0$ [7] or $\Theta \to \infty$, the network does not permit any spatial reuse. In this case, the transmit efficiency reduces to the efficiency of conventional slotted ALOHA [19], where for a network with N nodes, $p_{\text{opt}} = 1/N$ and $T_{\text{eff}} = \lim_{N\to\infty}(1 -$

[7] In fact, $\alpha \to 2$ is sufficient for infinite networks..

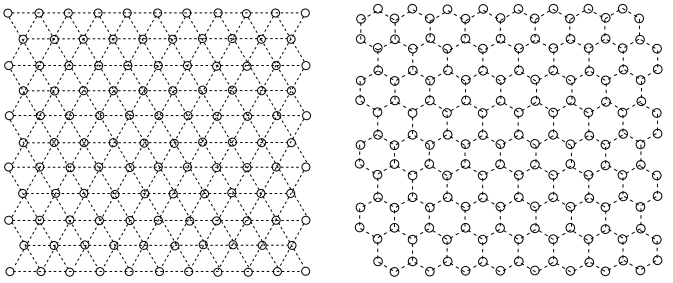

(a) Triangle Network (b) Hexagon network

Fig. 5. The topology of (a) triangle network and (b) hexagon network.

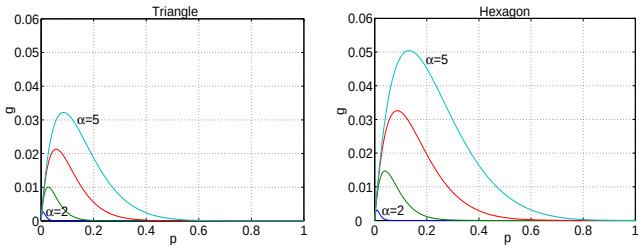

(a) (b)

Fig. 6. The analytic throughput $g(p)$ vs. p for two-dimensional networks with (a) triangle topology and (b) hexagon topology, where $\Theta = 10$ and $N = 1600$ nodes.

$1/N)^{N-1} = e^{-1}$ [4]. The fact that our limit coincides with the limit for conventional slotted ALOHA further validates our approximations. Note that while *Analytic 1* provides a better approximation, the other two methods yield closed-form expressions that are much more easily evaluated.

B. Triangle networks and hexagon networks

Some other regular topologies of interest are the triangle topology and its dual, the hexagon topology (Fig. 5). For each triangle, there are three vertices and six nearest neighbors for each vertex, while for the hexagon, there are six vertices for each hexagon and three nearest neighbors for each vertex. Again, the next-hop receiver of each packet is one of the nearest neighbor nodes of the transmitter, so the transmitter-receiver distance d_0 is equal to the side length of the regular polygon. In the triangle network, each node is located in a hexagon with area $\frac{\sqrt{3}}{2}d_0^2$. For node density is 1, $d_0 = \sqrt{\frac{2}{\sqrt{3}}}$. Similarly, for hexagon networks, $d_0 = \sqrt{\frac{4}{3\sqrt{3}}}$ for density 1.

The calculation of P_s in (6) depends on the geometry of the node placement. Similar to the derivation of square lattice networks as in (6), we get the relationship between the throughput g and the transmit probability p and compare the performance of triangle and hexagon networks in Fig. 6 (a), (b). To compare the performance of the three network, we introduce the *transport capacity* which can be defined as $Z := g_{max}d_0$. The comparison of square, triangle, and hexagon networks for $\alpha = 4$ is shown in Table II. The performance difference among the three topologies can be explained by the distance and number of the potential interfering nodes. Note that the transmit efficiency T_{eff} is very close to the one of conventional slotted ALOHA and does not depend on the topology.

TABLE II

COMPARISON OF SQUARE, TRIANGLE AND HEXAGON NETWORKS FOR $\alpha = 4$ AND $\Theta = 10$, WHERE p_{opt}, $g_{\max}$ AND T_{eff} DENOTE THE OPTIMUM TRANSMIT PROBABILITY, MAXIMUM THROUGHPUT AND TRANSMIT EFFICIENCY.

	p_{opt}	$g_{\max}$	T_{eff}	d_0	$g_{\max}d_0$
Square	0.0660	0.0247	0.37	1.0	0.0247
Triangle	0.0570	0.0213	0.37	1.0746	0.0229
Hexagon	0.0870	0.0326	0.37	0.8774	0.0286

IV. RANDOM NETWORKS

Here, we assume that the positions of the nodes constitute a Poisson point process. Note for large networks, this is equivalent to a uniformly random distribution for all practical purposes. For a given realization of a random network with $N = 1600$ nodes, Fig. 7 (a) displays the analytic throughput based on (5) for a node in the center

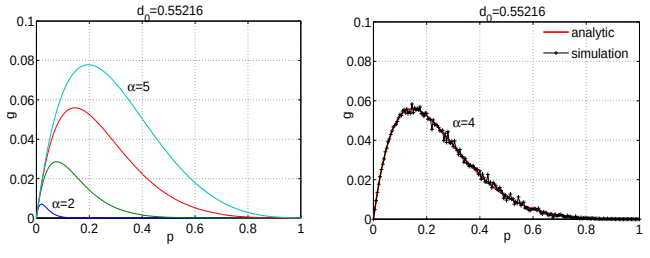

(a) (b)

Fig. 7. For a receiver node in the center of a fixed network realization with $N = 1600$ nodes around and $d_0 = 0.5522$, (a) analytic result of throughput g vs. transmit probability p based on equation (5) and (b) simulation result over 2000 runs comparing with analytic result for $\alpha = 4$ and $\Theta = 10$.

area with the transmitter-receiver distance $d_0 = 0.5522$. The simulation result of its throughput based on 2000 runs is compared with the analytic result for $\alpha = 4$ in Fig. 7 (b). It is shown that they match each other well.

In the following, we will investigate the throughput averaged over network realizations when the transmitter-receiver distance d_0 is fixed (Section IV-A) and not fixed (Section IV-B).

A. Average throughput for fixed d_0

In this case, we assume the distance between the desired transmitter and receiver is fixed and there are N other nodes constituting a two-dimensional Poisson point process. Although (5) gives the success probability conditioned on $d_1, d_2, \ldots, d_N$, we still need to find the joint density of $d_1, d_2, \ldots, d_N$ (ordered distances). It is well known that for one-dimensional Poisson point processes with density λ, the ordered distance from nodes to the desired receiver form the arrival times of a Poisson process [18]. The inter-arrival intervals are iid exponential with parameter λ

$$f_{d_i - d_{i-1}}(x_i - x_{i-1}) = \lambda e^{-\lambda(x_i - x_{i-1})}. \tag{17}$$

So for the ordered distance $0 \le d_1 \le \cdots \le d_N$, the joint density function of the inter-arrival intervals is

$$\begin{aligned} &f_{d_1, d_2, \cdots, d_N}(x_1, x_2, \cdots, x_N) \\ =&f_{d_1, \cdots, d_N - d_{N-1}}(x_1, x_2 - x_1, \cdots, x_N - x_{N-1}) \\ =&\left(\lambda e^{-\lambda x_1}\right)\left(\lambda e^{-\lambda(x_2 - x_1)}\right) \cdots \left(\lambda e^{-\lambda(x_N - x_{N-1})}\right) \\ =&\lambda^N e^{-\lambda x_N}, \qquad 0 \le x_1 \le x_2 \le \cdots \le x_N \end{aligned} \tag{18}$$

When nodes are distributed according to a two-dimensional Poisson point process with density λ, the squared ordered distances from the desired receiver have the same distribution as the arrival times of a Poisson process with density $\lambda\pi$ [18]. The squared ordered distances have a joint distribution with density

$$\begin{aligned} f_{d_1^2, \cdots, d_N^2}(x_1, \cdots, x_N) = (\lambda\pi)^N e^{-\lambda\pi x_N}, \\ 0 \le x_1 \le x_2 \le \cdots \le x_N, \end{aligned} \tag{19}$$

because from [20], we have

$$f_{d_i^2 - d_{i-1}^2}(x_i - x_{i-1}) = \lambda\pi e^{-\lambda\pi(x_i - x_{i-1})}. \tag{20}$$

The conditional success probability can be written as (see (5))

$$P_{s|d_0, d_1, \cdots, d_N} = \prod_{i=1}^{N} \frac{(d_i^2)^{\frac{\alpha}{2}} + (1-p)\Theta d_0^\alpha}{(d_i^2)^{\frac{\alpha}{2}} + \Theta d_0^\alpha}. \tag{21}$$

Integrating (21) with respect to the joint density (19), and in particular, evaluating it for $\alpha = 4$, we obtain

$$\begin{aligned} P_{s|d_0} = \int_0^\infty (\lambda\pi)^N e^{-\lambda\pi x_N} \Big\{ \int_0^{x_N} \cdots \int_0^{x_2} \\ \prod_{i=1}^{N} \frac{x_i^2 + (1-p)\Theta d_0^4}{x_i^2 + \Theta d_0^4} \mathrm{d}x_1 \cdots \mathrm{d}x_{N-1} \Big\} \mathrm{d}x_N. \end{aligned} \tag{22}$$

By applying a similar inductive technique as in [18], it can be shown that

$$\begin{aligned} &\int_0^{x_N} \cdots \int_0^{x_2} \prod_{i=1}^{N-1} \frac{x_i^2 + (1-p)\Theta d_0^4}{x_i^2 + \Theta d_0^4} \mathrm{d}x_1 \cdots \mathrm{d}x_{N-1} \\ =&\frac{1}{(N-1)!}\left(x_N - p\sqrt{\Theta d_0^4}\arctan\left(\frac{x_N}{\sqrt{\Theta d_0^4}}\right)\right)^{N-1}. \end{aligned} \tag{23}$$

Combining (22) and (23), we have

$$\begin{aligned} P_{s|d_0} = \int_0^\infty \frac{(\lambda\pi)^N}{(N-1)!} e^{-\lambda\pi x} \frac{x^2 + (1-p)\Theta d_0^4}{x^2 + \Theta d_0^4} \\ \left(x - p\sqrt{\Theta d_0^4}\arctan\left(\frac{x}{\sqrt{\Theta d_0^4}}\right)\right)^{N-1} \mathrm{d}x. \end{aligned} \tag{24}$$

Based on (24), we numerically evaluate the average throughput $\mathbb{E}[g|d_0] = p(1-p)P_{s|d_0}$ (averaged over all network realizations) and plot it as a function of p in Fig. 8 (a) for a network with node numbers $N = 100$, 121 and 144, where $d_0 = 1$. It is shown that they are very close, indicating that only a portion of nodes interferes at the receiver and that nodes further away have little impact on the transmission. Fig. 8 (b) compares the analytical average throughput $\mathbb{E}[g|d_0]$ (dashed line) according to equation (24) with the simulation result of the throughput for center link with $d_0 = 1$ averaged over 10000 network realizations (marked by $+$). Note that the analytical approach used to derive (23) is restricted to $\alpha = 4$. Luckily, this value of α is of significant practical relevance [21]. For other values of α, one has to resort to simulation.

B. Average throughput for variable d_0

In the previous analysis, we assumed the transmitter-receiver distance d_0 is fixed and N potential interfering nodes are uniformly distributed around. Now we assume that the receiver located at the center selects its nearest neighbor node as its desired transmitter. Then there are $N - 1$ nodes further away than the desired transmitter.

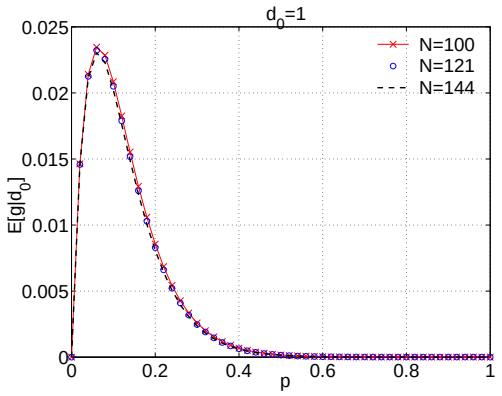

(a)

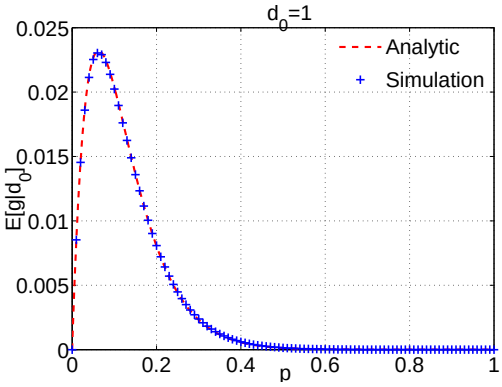

(b)

Fig. 8. For $\alpha = 4$ and $\Theta = 10$, (a) The analytical average throughput $\mathbb{E}[g|d_0 = 1]$ based on equation (24) for networks with node number $N = 100$, 121 and 144. (b) Comparison of the analytical average throughput $\mathbb{E}[g|d_0 = 1]$ (dashed line) with the simulation result for the center link over 10000 network realizations ($+$ mark), where the receiver has $N = 144$ potential interfering nodes around.

The distance to the nearest neighbor has the Rayleigh density function (as shown in [15]):

$$f_{d_0}(x) = 2\pi x e^{-\pi x^2}. \tag{25}$$

Since d_0 is the nearest distance, d_i^2 in (21) can be varying from d_0^2 to d_{i+1}^2. So we integrate x_i from d_0^2 to x_{i+1}:

$$P_{s|d_0} = \int_{d_0^2}^{\infty} f_{d_1^2,\ldots,d_{N-1}^2|d_0^2}(x_1,\ldots,x_{N-1}|d_0^2)\Big\{\int_{d_0^2}^{x_{N-1}} \cdots \int_{d_0^2}^{x_2} \prod_{i=1}^{N-1} \frac{x_i^2 + (1-p)\Theta d_0^4}{x_i^2 + \Theta d_0^4} \mathrm{d}x_1 \ldots \mathrm{d}x_{N-2}\Big\}\mathrm{d}x_{N-1} \tag{26}$$

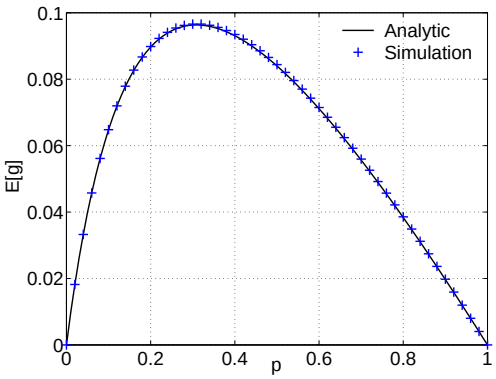

Fig. 9. For $\alpha = 4$ and $\Theta = 10$, $\mathbb{E}[g]$ vs. p for random network with $N = 144$. The analytic result from (26) and (29) is displayed by solid line; the simulation result over 10000 runs by $+$ mark.

and

$$f_{d_1^2,\ldots,d_{N-1}^2|d_0^2}(x_1,\ldots,x_{N-1}|d_0^2) = (\lambda\pi)^{N-1} e^{-\lambda\pi(x_{N-1}-d_0^2)}, \quad \text{where } 0 \le d_0^2 \le x_1 \le \cdots \le x_{N-1}. \tag{27}$$

By induction, it can be shown that

$$\int_{d_0^2}^{x_{N-1}} \cdots \int_{d_0^2}^{x_2} \prod_{i=1}^{N-2} \frac{x_i^2 + (1-p)\Theta d_0^4}{x_i^2 + \Theta d_0^4} \mathrm{d}x_1 \ldots \mathrm{d}x_{N-2} = \frac{1}{(N-2)!}\Big\{x_{N-1} - d_0^2 - p\sqrt{\Theta d_0^4} \cdot \Big[\arctan\Big(\frac{x_{N-1}}{\sqrt{\Theta d_0^4}}\Big) - \arctan\Big(\frac{d_0^2}{\sqrt{\Theta d_0^4}}\Big)\Big]\Big\}^{N-2}. \tag{28}$$

The success probability averaged over d_0 is given by:

$$P_s = \int_0^{\infty} f_{d_0}(x) P_{s|d_0} \mathrm{d}x \tag{29}$$

Substitute (27) and (28) into (26) and evaluate (29) with (25), we obtain the relationship between $\mathbb{E}[g] = p(1-p)P_s$ and p, which is plotted in Fig. 9. It is shown that the analytic (solid line) and simulation result (marked by $+$) match each other perfectly.

Fig. 9 implies random networks have better average throughput for local data exchange than regular networks. This can be explained by d_0, the transmitter-receiver distance. In random networks, a variable d_0 leads to a variable throughput. Fig. 10 (a) displays $\mathbb{E}[g|d_0]$ vs. p for d_0 from 0.5 to 1.5. Fig. 10 (b) shows the relationship for $d_0 = 0.1$, 0.5, 1.0 and 1.5. Not surprisingly, smaller d_0 results in higher throughput. For the variable d_0 case, it is assumed that the desired transmitter is the nearest neighbor of the receiver. With

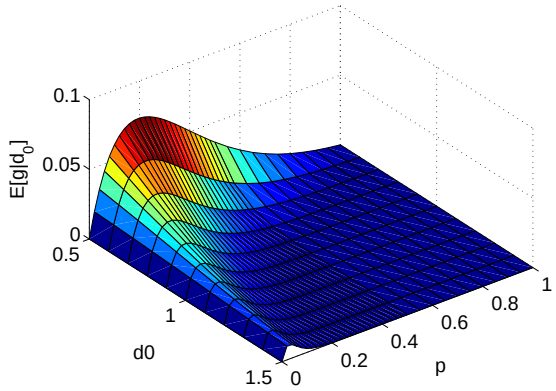

(a)

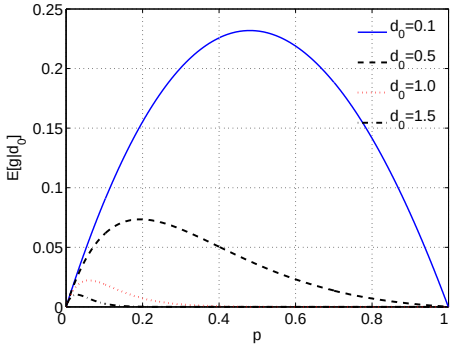

(b)

Fig. 10. For $\alpha = 4$ and $\Theta = 10$, average throughput (a) $\mathbb{E}[g|d_0]$ vs. p for d_0 from 0.5 to 1.5. (b) $\mathbb{E}[g|d_0]$ vs. p for $d_0 = 0.1$, 0.5, 1.0 and 1.5.

the pdf of (25), the probability that d_0 is greater than 1 (the inter-node distance in square regular network) is $\mathbb{P}[d_0 > 1] = e^{-\pi} = 0.043$. So for most nodes, the received signal power from the desired transmitter is greater than that in regular networks. In Fig. 10 (b), for $d_0 = 0.1$, it is shown that the strong signal power resulting from very small d_0 offsets the impact of interference even for high transmit probabilities p.

Now consider the generic routing strategy from [15]: each node in the path sends packets to its nearest neighbor that lies within a sector ϕ, i.e., within $\pm\phi/2$ of the source-destination direction. The previous scheme where d_0 is obtained as the distance to the nearest neighbor makes no progress in the source-destination direction. Such a choice of d_0 would correspond to routing within $\phi = 2\pi$, clearly an inefficient choice of ϕ. More sensible is $\phi \leq \pi$. Let d_0 be the distance to the nearest neighbor

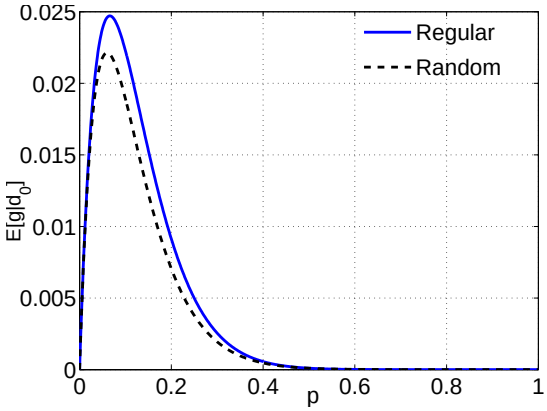

Fig. 11. Comparison of the average throughput of regular square network and random network. For both networks, $N = 1600$, $d_0 = 1$, $\alpha = 4$ and $\Theta = 10$.

within sector ϕ. The probability density of d_0 is given by [15]:

$$f_{d_0}(x) = x\phi e^{-x^2\phi/2}. \tag{30}$$

If the routing sector $\phi = \pi/2$, then $\mathbb{E}[d_0] = 1$. For $d_0 = 1$, Fig. 11 displays the throughput for square network and random network with $N = 1600$. It turns out that for the same transmitter-receiver distance, square networks have a slightly higher average throughput than random networks.

We compare the transport capacity $g_{\max}d_0$ of regular and random networks. Fig. 12 (a) shows $g_{\max}$ vs. d_0 and p_{opt} vs. d_0 for a random network. Fig. 12 (b) compares the transport capacity of random and regular networks. It is shown that at a specific transmitter-receiver distance d_0, regular networks slightly outperform random networks in terms of transport capacity.

C. End-to-end throughput g_{EE} in a random network

In wireless sensor networks with multihop communication, the end-to-end throughput (the minimum of the throughput values of the nodes involved) of a route with an average number of hops is a better performance indicator than the average throughput. For two-dimensional random sensor networks (area $m \times m$, density 1, routing within sector ϕ) with uniformly randomly selected source and fixed destination located at the corner[8], we can approximate the average path length in hops

$$\bar{h} \approx \frac{\bar{r}}{\bar{D}\eta}. \tag{31}$$

[8]For the many-to-one traffic typical in sensor networks, we assume the data sink for all connections to be in one of the corners of the (square) network.

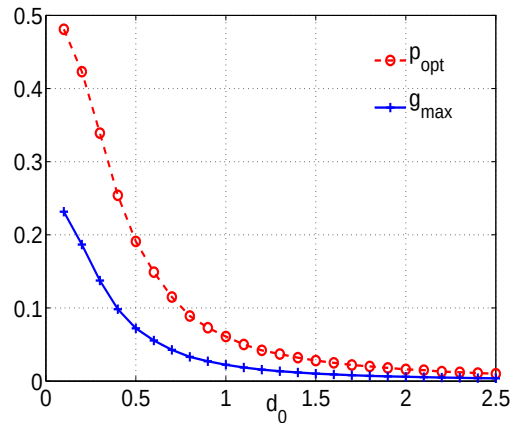

(a)

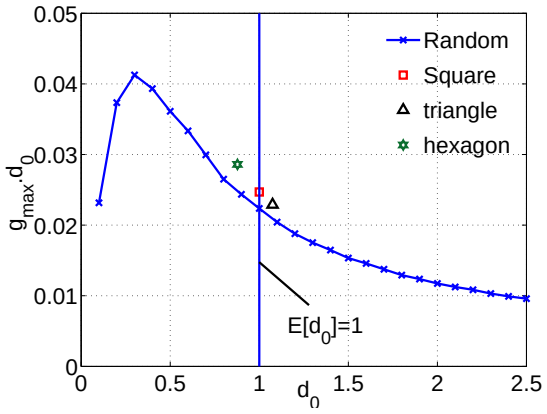

(b)

Fig. 12. With $N = 1600$, $\alpha = 4$ and $\Theta = 10$, (a) $g_{\max}$ vs. d_0 and p_{opt} vs. d_0 for a random network, (b) transport capacity $g_{\max} d_0$ for random and regular networks with the same size and node density. For random networks, $\mathbb{E}[d_0] = 1$ for $\phi = \pi/2$.

where $\bar{r}$ denotes the expected distance between the source-destination pair, $\bar{D}$ the expected hop length and η the expected path efficiency, where the path efficiency is the ratio between the Euclidean distance and the travelled distance of a path. $\bar{D}\eta$ can be viewed as the effective hop length — the average hop length projected in the desired source-destination direction. The mean distance from a random point in a square to a corner can be derived from [22, Exercise 2.4.5]:

$$\bar{r} = \left[\frac{\sqrt{2}}{3} + \frac{1}{3} \text{arctanh}(\frac{1}{\sqrt{2}}) \right] m \approx 0.769m, \qquad (32)$$

From [15], we know that

$$\bar{D} = \sqrt{\frac{\pi}{2\phi}}, \qquad \eta = \frac{2}{\phi} \sin(\frac{\phi}{2}). \qquad (33)$$

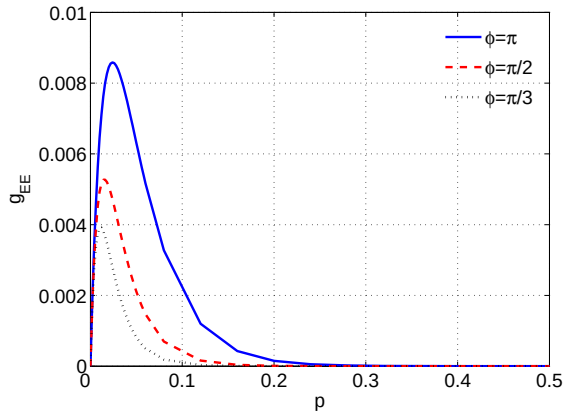

Fig. 13. The average end-to-end throughput of random networks for different routing sectors ϕ, where $\alpha = 4$ and $\Theta = 10$.

So the average path length in hops can be approximated by plugging (32) and (33) into (31). To evaluate the end-to-end throughput of a route with $\bar{h}$ hops, we use a semi-analytic approach by generating an $\bar{h}$-hop path with each hop length obtained as a realization of D according to pdf in (30), and evaluate the throughput of each hop based on Fig. 10 (a). The average end-to-end throughput is then obtained by taking the minimum of each path and averaging the minimum over the number of realizations of the simulated routes. Fig. 13 shows that the maximum end-to-end throughput g_{EE} is 0.0086, 0.0053 and 0.0039 for $\phi = \pi$, $\pi/2$ and $\pi/3$.

What is the end-to-end throughput for regular networks? It can be directly obtained from Fig. 2 (a) and Fig. 6, which is 0.0247, 0.0213 and 0.0326 for square, triangle and hexagon networks. For regular networks, every hop has the same length, and the throughput is calculated for a node in the center of the network, which is the worst case, so the end-to-end throughput (minimum throughput of all the nodes involved) is the throughput of the center node. In terms of the end-to-end throughput for multihop communication, regular networks significantly outperform random networks. For larger networks, the benefit is larger since larger m results in longer paths.

V. Conclusions

We have shown that for a noiseless Rayleigh fading network with slotted ALOHA, the success probability of a transmission is the Laplace transform of the interference evaluated at the SIR threshold Θ. Even though for sensor networks, more elaborate MAC schemes might be used in practice, the analysis for slotted ALOHA

provides lower bounds of the performance for other MAC schemes and can serve as a benchmark.

Among the three regular networks (square, triangle, hexagon), the hexagon network provides the highest throughput since every node has only three nearest neighbors which is the smallest number among the three networks. The analysis of the dependence of the maximum throughput $g_{\max}$ and optimum transmit probability p_{opt} on Θ for square networks shows that the transmit efficiency $T_{\text{eff}} = g_{\max}/p_{\text{opt}}$ varies from e^{-1} to $1/2$ as the spatial reuse increases from 0 to ∞. In practical networks ($\alpha/\Theta < 1$) that are optimized for throughput, the spatial reuse does not permit a transmit efficiency close to $1/2$. So, in most cases, it will be closer to e^{-1}, which implies that at maximum throughput, the packet loss rate is about 60%, which is surprisingly high. These results hold quantitatively for the other two regular networks — triangle and hexagon networks.

For random networks, two scenarios are considered — fixed and variable transmitter-receiver distance d_0. In the latter case, the throughput is averaged over the actual distribution of the nearest-neighbor distance d_0. Conditioned on d_0 being the same for random and regular networks, regular networks slightly outperform random networks in terms of (per-node) throughput and transport capacity. In the case of variable d_0 where the receiver selects the nearest neighbor node as its desired transmitter, the average throughput of random networks is better than that of regular ones. This is because strong signal powers resulting from very small d_0 offset the impact of interference even for high transmit probabilities. This result, however, only pertains to local data exchange. When multihop communication and effective routing is taken into account, regular topologies have a significant advantage in terms of end-to-end throughput.

REFERENCES

[1] I. F. Akyildiz, W. Su, Y. Sankarasubramaniam, and E. Cayirci, "Wireless sensor networks: a survey," *Computer Networks*, vol. 38, no. 4, pp. 393–422, Mar. 2002.

[2] P. Gupta and P. R. Kumar, "The Capacity of Wireless Networks," *IEEE Transactions on Information Theory*, vol. 46, no. 2, pp. 388–404, Mar. 2000.

[3] S. Toumpis and A. J. Goldsmith, "Capacity Regions for Wireless Ad Hoc Networks," *IEEE Transactions Wireless Communications*, vol. 2, no. 4, pp. 736–748, July 2003.

[4] J. A. Silvester and L. Kleinrock, "On the Capacity of Multihop Slotted ALOHA Networks with Regular Structure," *IEEE Transactions on Communications*, vol. COM-31, no. 8, pp. 974–982, Aug. 1983.

[5] M. Grossglauser and D. Tse, "Mobility Increases the Capacity of Ad-hoc Wireless Networks," in *IEEE INFOCOM*, Anchorage, AL, 2001.

[6] L. Xie and P. R. Kumar, "A Network Information Theory for Wireless Communication: Scaling Laws and Optimal Operation," *IEEE Transactions on Information Theory*, vol. 50, no. 5, pp. 748–767, May 2004.

[7] S. De, C. Qiao, D. A. Pados, and M. Chatterjee, "Topological and MAI Constraints on the Performance of Wireless CDMA Sensor Networks," in *Proceedings of IEEE INFOCOM*, Hongkong, Mar. 2004.

[8] G. Ferrari and O. K. Tonguz, "Performance of Ad Hoc Wireless Networks with Aloha and PR-CSMA MAC protocol," in *Proc. IEEE Glob. Telecommun. Conf. (GLOBECOM'03)*, San Francisco, CA, Dec. 2003, pp. 2824–2829.

[9] S. Panichpapiboon, G. Ferrari, and O. K. Tonguz, "Sensor Networks with Random Versus Uniform Topology: MAC and Interference Considerations," in *Proc. IEEE Veh. Tech. Conf., (VTC Spring'04)*, Milan, Italy, May 2004.

[10] IEEE Trans. On Veh.Tech. Vol. VT-37, 1988. Special issue on radio propagation.

[11] A. J. Goldsmith and S. B. Wicker, "Design Challenges for Energy-Constrained Ad Hoc Wireless Networks," *IEEE Wireless Communications*, vol. 9, no. 4, pp. 8–27, Aug. 2002.

[12] A. Ephremides, "Energy Concerns in Wireless Networks," *IEEE Wireless Communications*, vol. 9, no. 4, pp. 48–59, Aug. 2002.

[13] A. Woo, T. Tong, and D. Culler, "Taming the Underlying Challenges of Reliable Multihop Routing in Sensor Networks," in *Proceedings of the First International Conference on Embedded Networked Sensor Systems*, Los Angeles, CA, Nov. 2003.

[14] E. S. Sousa and J. A. Silvester, "Optimum Transmission Ranges in a Direct-Sequence Spread-Spectrum Multihop Packet Radio Network," *IEEE Journal on Selected Areas in Communications*, vol. 8, no. 5, pp. 762–771, June 1990.

[15] M. Haenggi, "On Routing in Random Rayleigh Fading Networks," *IEEE Transactions on Wireless Communications*, July 2005, available at http://www.nd.edu/~mhaenggi/routing.pdf.

[16] J.-P. M. G. Linnartz, "Exact Analysis of the Outage Probability in Multiple-User Radio," *ieeecomm*, vol. 40, no. 1, pp. 20–23, Jan. 1992.

[17] F. Baccelli, B. Blaszczyszyn, and P. Mühlethaler, "A Spatial Reuse Aloha MAC Protocol for Multihop Wireless Mobile Networks," Institut National de Recherche en Informatique et en Automatique (INRIA), Rocquencourt, Le Chesnay Cedex, France, Tech. Rep. 4955, Oct. 2003, available at http://www.terminodes.org/MV2003-Present/Me15/Spacial-Baccelli.pdf.

[18] R. Mathar and J. Mattfeldt, "On the Distribution of Cumulated Interference Power in Rayleigh Fading Channels," *Wireless Networks 1*, no. 1, pp. 31–36, Feb. 1995.

[19] N. Abramson, "The Aloha System - Another Alternative for Computer Communications," *Proceedings of Fall Joint Computer Conference, AFIPS Conference*, 1970.

[20] M. Hellebrandt and R. Mathar, "Cumulated Interference Power and Bit-error-rates in Mobile Packet Radio," *Wireless Networks*, vol. 3, no. 3, pp. 169–172, 1997.

[21] T. S. Rappaport, *Wireless Communications – Principles and Practice*, 2nd ed. Prentice Hall, 2002, iSBN 0-13-042232-0.

[22] A. M. Mathai, *An Introduction to Geometrical Probability*. Gordon and Breach Science Publishers, 1999, ISBN 90-5699-681-9.